

Fluctuation and Noise Letters  
 © World Scientific Publishing Company

## THE OFF-RESONANT RATCHET: A STUDY OF THE CROSSOVER BETWEEN CLASSICAL AND QUANTUM DYNAMICS

R. K. SHRESTHA<sup>†</sup>, W. K. LAM, J. NI, and G. S. SUMMY

*Department of Physics, Oklahoma State University,  
 Stillwater, Oklahoma 74078-3072, USA*

<sup>†</sup>*rajendra.shrestha@okstate.edu*

We study the crossover between classical and quantum dynamics by observing the behavior of a quantum ratchet created by exposing a Bose-Einstein condensate to short pulses of a potential which is periodic in both space and time. Such a ratchet is manifested by a directed current of particles, even though there is an absence of a net bias force. We confirm that the ratchet behavior can under certain circumstances be the same in both regimes. We demonstrate that this behavior can be understood using a single variable containing many of the experimental parameters and thus the ratchet current is describable using a single universal scaling law.

### 1. Introduction

Understanding the nature of the crossover between classical and quantum behavior is one of the most important unresolved problems in physics. One place where the stark difference between the two paradigms becomes very clear is in classical non-linear systems. Classically, such a system can exhibit chaos in which it is effectively impossible to predict its long term evolution, while in contrast because of the linearity of the Schrodinger equation, an equivalent quantum mechanical systems is completely deterministic. One of the systems of choice for studying this behavior is the so-called delta-kicked rotor, typically realized with a sample of cold or ultra-cold atoms kicked by short pulses of an optical standing wave This is the atom optics quantum kicked rotor (AOQKR) [1]. While theory and experiment has been successful in elucidating some features of this and similar systems, there are still many aspects that remain to be discovered. Ever since its realization, it has been one of the workhorses for studies of experimental quantum chaos. It has revealed a wide variety of interesting effects including: dynamical localization [2], quantum resonances (QRs) [2–4], quantum accelerator modes [5, 6], and quantum ratchets [7–15]. The latter are quantum mechanical systems that display directed motion of particles in the absence of unbalanced forces. They are of considerable interest because classical ratchets are the underlying mechanism for some biological motors and nanoscale devices [10]. Recent theoretical [11, 13] and experimental [8] studies have demonstrated that a controllable directed current arises in kicked atom

systems at QR. A QR occurs when the kicking period is commensurate with the natural periods of the rotor and is characterized by a quadratic growth of the kinetic energy with time. The question of what happens to a ratchet away from resonance was addressed in a recent theoretical paper [16]. In that work, the authors developed a classical-like ratchet theory and proposed the existence of a one-parameter scaling law that could be used to predict the ratchet current for a wide variety of parameters. It was also shown that an inversion of the momentum current is possible for some sets of scaling variables. This was experimentally verified in Ref. [17].

In this paper, we report on the ratchet current behavior in the true classical and also at the so-called  $\epsilon$ -classical regimes, verifying that in both cases, it behaves in essentially the same way. It is shown that the ratchet current exhibits an inversion (negative current) for certain families of experimental parameters. We demonstrate that this can be explained by a scaling law when the ratchet is close to the classical limit or one of the QRs. The effect of the initial momentum width of the atomic distribution on the off-resonant ratchet is also investigated.

## 2. Theory

The dynamics of the AOQKR system can be described by a Hamiltonian which in dimensionless units is [5, 18, 19]:  $\hat{\mathcal{H}} = \frac{\hat{p}^2}{2} + \phi_d \cos(\hat{X}) \sum_{q=1}^t \delta(t' - q\tau)$ , where  $\hat{p}$  is the momentum (in units of  $\hbar G$ , two photon recoils) that an atom of mass  $M$  acquires from short, periodic pulses of a standing wave with a grating vector  $G = 2\pi/\lambda_G$  ( $\lambda_G$  is the spatial period of the standing wave). Since momentum in this system is only changed in quanta of  $\hbar G$ , we break down  $p$  as  $p = n + \beta$  where  $n$  and  $\beta$  are integer and fractional parts of the momentum respectively and  $\beta$ , the quasi-momentum, is conserved. Other variables are the position  $\hat{X}$  (in units of  $G^{-1}$ ), the continuous time variable  $t'$  (integer units), and the kick number  $q$ . The pulse period  $T$  is scaled by  $T_{1/2} = 2\pi M/\hbar G^2$  (the half-Talbot time) to give the scaled pulse period  $\tau = 2\pi T/T_{1/2}$ . The strength of the kicks is given by  $\phi_d = \Omega^2 \Delta t / 8\delta_L$ , where  $\Delta t$  is the pulse length,  $\Omega$  is the Rabi frequency, and  $\delta_L$  is the detuning of the kicking laser from the atomic transition. To create a ratchet from this Hamiltonian it was shown in [8] that a superposition of two plane waves should be used for the initial state.

A successful approach to treating this system close to resonant values of  $\tau$  (i.e.  $\tau = 2\pi\ell$ , with  $\ell > 0$  integer) is the so called  $\epsilon$ -classical theory. Here the scaled pulse period is written as  $\tau = 2\pi\ell + \varepsilon$ , where  $|\varepsilon| \ll 1$ , and can be shown to play the role of Planck's constant. In this case the dynamics can be understood by the classical mapping [5, 19],

$$J_{q+1} = J_q + \tilde{k} \sin(\theta_{q+1}), \quad \theta_{q+1} = \theta_q + J_q, \quad (1)$$

where  $\tilde{k} = |\varepsilon|\phi_d$  is the scaled kicking strength,  $J_q = \varepsilon p_q + \ell\pi + \tau\beta$  is the scaled momentum variable and  $\theta_q = X \bmod (2\pi) + \pi[1 - \text{sign}(\varepsilon)]/2$  is the scaled position exploiting the spatial periodicity of the kick potential. As mentioned above, for the

ratchet we start with a superposition of plane waves  $|\psi_0\rangle = \frac{1}{\sqrt{2}} [ |0\hbar G\rangle + e^{i\gamma} |1\hbar G\rangle ]$ , or equivalently a rotor state  $\frac{1}{\sqrt{4\pi}} [1 + e^{i(\theta+\gamma)}]$ . This leads to the position space probability distribution function  $P(\theta) = |\psi(\theta)|^2 = \frac{1}{2\pi} [1 + \cos(\theta + \gamma)]$ . Here  $\gamma$  is an additional phase used to account for the possibility that the initial spatial atomic distribution is shifted in position relative to the applied periodic potential. Although the distribution  $P(\theta)$  is quantum in origin, in what follows it will be interpreted as a classical probability.

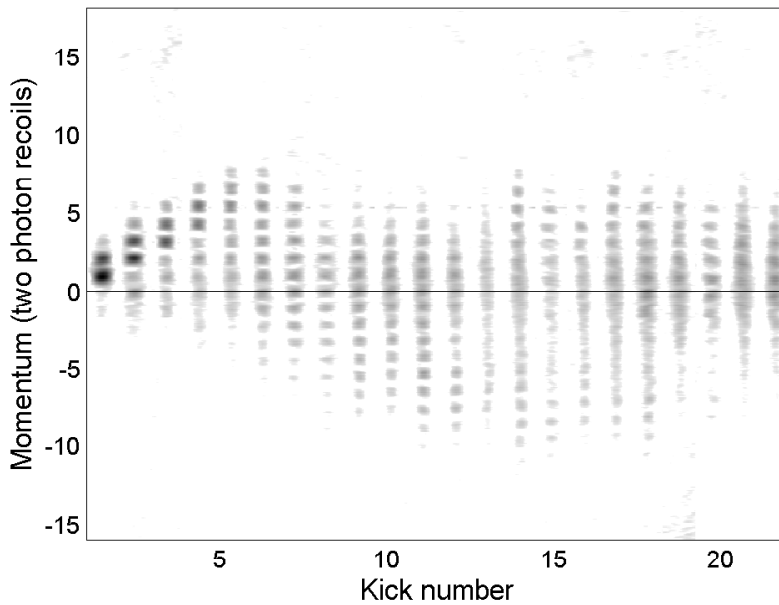


Fig. 1. Experimental momentum distributions after exposing a BEC to short pulses of an off-resonant standing wave of light. The momentum distributions are shown as a function of kick number ( $\ell = 1$ ,  $|\varepsilon| = 0.18$ ,  $\phi_d = 1.8$  and  $\gamma = -\pi/2$ ). Each momentum distribution was captured in a separate time-of-flight experiment.

The original application of  $\varepsilon$ -classical theory to the kicked rotor system showed the existence of a one-parameter scaling law for the mean energy [20]. This was experimentally verified in the vicinity of the first and second quantum resonances ( $\ell = 1$  and  $\ell = 2$ ) in Ref. [21]. It was found that the scaled energy could be written as  $\frac{E}{\phi_d^2 q} = 1 - \Phi_0(x) + \frac{4}{\pi x} G(x)$  where  $x = \sqrt{\phi_d |\varepsilon|} q$  is a scaling variable and  $\Phi_0(x)$  and  $G(x)$  are closed form functions of  $x$ . Recently, the existence of a one-parameter scaling law for the ratchet current using the same scaling parameter  $x$  was proposed [16]. One of the notable features of this theory is that it predicts

that at some values of the scaling variable (i.e. certain families of real parameters) an inversion of momentum current can occur.

In the pendulum approximation [22], the motion of the kicked rotor in continuous time is described by the scaled Hamiltonian  $H' \approx (J')^2/2 + |\varepsilon|\phi_d \cos(\theta)$ . Here  $J' = J/(\sqrt{\phi_d|\varepsilon|})$  is a scaled momentum variable. Near the quantum resonance, using the position space probability distribution function  $P(\theta)$ , one can calculate  $\langle J' - J'_0 \rangle = \int_{-\pi}^{\pi} d\theta_0 P(\theta_0)(J' - J'_0)$ . For  $|\varepsilon| \lesssim 1$ , Eq. (1) gives a phase space dominated by a pendulum-like resonance island of extension  $4\sqrt{k} \gg |\varepsilon|$  [20]. Hence  $p = 0$  and  $p = 1$  essentially contribute in the same way giving  $J'_0 = 0$  so that the map in Eq. (1) is  $J'_{q+1} = \sqrt{k} \sum_{q=0}^{t-1} \sin(\theta_{q+1})$ . With the scaling variable  $x$ , the average scaled momentum becomes  $\langle J' - J'_0 \rangle = -\sin \gamma F(x)$ , where

$$F(x) = \frac{1}{2\pi} \int_{-\pi}^{\pi} \sin \theta_0 J'(\theta_0, J'_0 = 0, x) d\theta_0. \quad (2)$$

Thus the mean momentum (units of  $\hbar G$ ) expressed in terms of the scaled variables is

$$\begin{aligned} \langle p \rangle &= \sqrt{\frac{\phi_d}{|\varepsilon|}} \langle J' - J'_0 \rangle = -\frac{\phi_d q \sin \gamma}{x} F(x) \\ \frac{\langle p \rangle}{-\phi_d q \sin \gamma} &= \frac{F(x)}{x} \end{aligned} \quad (3)$$

where  $F(x)$  can be computed from the above pendulum approximation [16].

### 3. Experiments

We performed our experiments using a similar set up to that described in [18]. A BEC of about 40000  $^{87}\text{Rb}$  atoms was created in the  $5S_{1/2}$ ,  $F = 1$  level using an all-optical trap technique [23]. Approximately 5 ms after being released from the trap, the condensate was exposed to a pulsed horizontal standing wave of wavelength  $\lambda_G$ . This was formed by two laser beams of wavelength  $\lambda = 780$  nm, detuned 6.8GHz to the red of the atomic transition. The direction of each beam was aligned at  $53^\circ$  to the vertical to give  $\lambda_G = \lambda/(2 \sin 53^\circ)$ . With these parameters the primary QR (half-Talbot time [3,24,25]) occurred at multiples of  $51.5 \pm 0.05 \mu\text{s}$ . Each laser beam was passed through an acousto-optic modulator driven by an arbitrary waveform generator. This enabled control of the phase, intensity, and pulse length as well as the relative frequency between the kicking beams. Adding two counterpropagating waves differing in frequency by  $\Delta f$  results in a standing wave that moves with a velocity  $v = 2\pi\Delta f/G$ . The initial momentum or quasi-momentum  $\beta$  of the BEC relative to the standing wave is proportional to  $v$ , so that by changing  $\Delta f$  the value of  $\beta$  could be systematically controlled. The kicking pulse length was fixed at  $1.54 \mu\text{s}$ , so we varied the intensity rather than the pulse length to change the kicking strength  $\phi_d$ . This was done by adjusting the amplitudes of the RF waveforms driving

the kicking pulses, ensuring that the experiments were performed in the Raman-Nath regime (the distance an atom travels during the pulse is much smaller than the period of the potential). The initial state for the experiment was prepared as

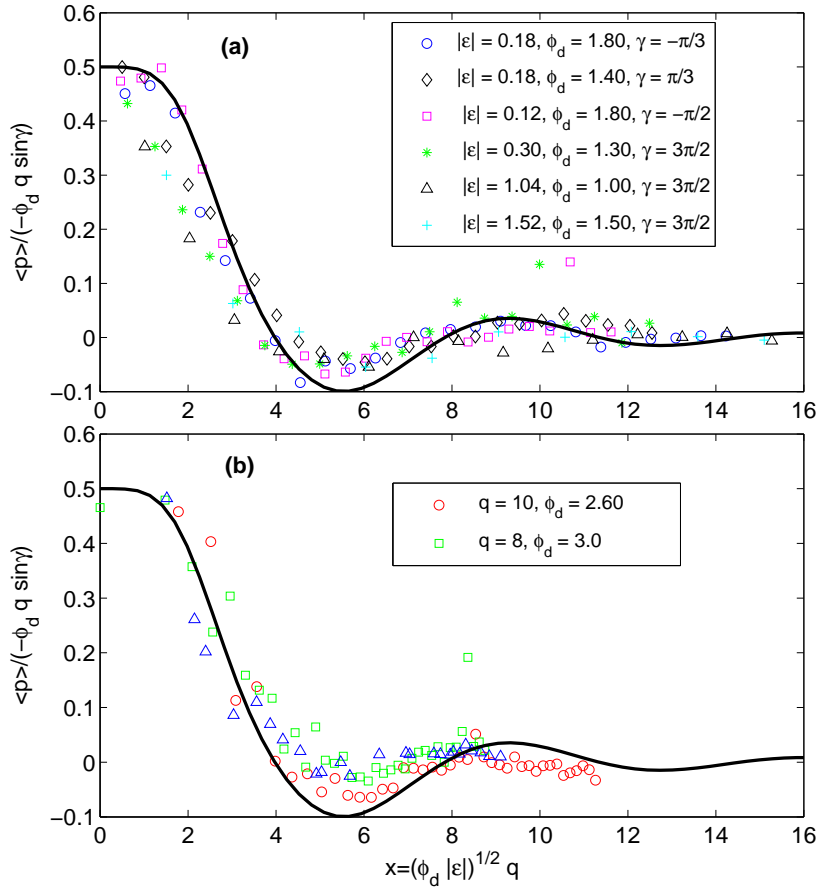


Fig. 2. Scaled mean momentum  $\langle p \rangle / (-\phi_d q \sin \gamma)$  as a function of the scaling variable  $x = \sqrt{(\phi_d |\varepsilon|)} q$  for  $\ell = 1$ . In (a)  $x$  was varied by scanning over kick number for different combinations of  $\phi_d$ ,  $|\varepsilon|$  and  $\gamma$ . In panel (b)  $x$  was varied by scanning over  $|\varepsilon|$  with  $q = 8$ ,  $\phi_d = 3.0$  (green squares), and with  $q = 10$ ,  $\phi_d = 2.6$  (red circles). Also plotted in (b) is data from a scan over  $\phi_d$  with  $|\varepsilon| = 0.18$ ,  $q = 8$  (blue triangles). In both panels, the solid line is the function  $F(x)/x$  given by Eq. (3). This demonstrates that no matter how  $x$  is obtained the scaled mean momentum is approximately universal.

a superposition of two momentum states  $|p = 0\hbar G\rangle$  and  $|p = 1\hbar G\rangle$  by applying a long ( $\Delta t = 38.6\mu s$ ) and very weak standing wave pulse (Bragg pulse). By using a

pulse of suitable strength, an equal superposition of the two aforementioned atomic states was created ( $\pi/2$  pulse). The Bragg pulse was immediately followed by the kicking pulses in which a relative phase of  $\gamma$  between the beams was applied. This phase was experimentally controlled by adjusting the phase difference between the RF waveforms driving the two AOMs. Finally the kicked atoms were absorption imaged after 9 ms using a time-of-flight measurement technique to yield momentum distributions like those seen in Fig. 1. A detailed examination of this data shows that the momentum distributions initially tend strongly towards positive momenta, followed by current reversal regions around 15 kicks where the distributions tend negative. This is evidence of the current inversion predicted by Eq. (3).

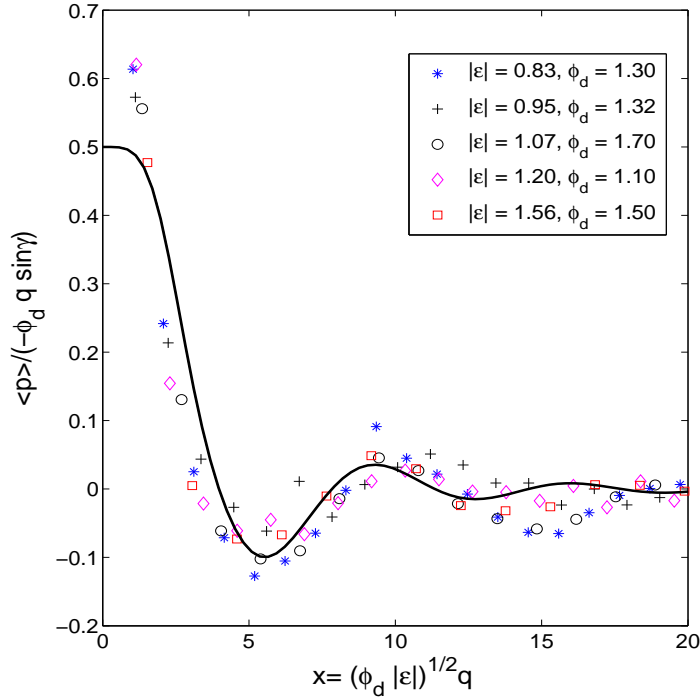


Fig. 3. Scaled mean momentum  $\langle p \rangle / (-\phi_d q \sin \gamma)$  as a function of the scaling variable  $x = \sqrt{(\phi_d |\epsilon|)} q$  for  $\ell = 0$ .  $x$  was varied by scanning over kick number for different combinations of  $\phi_d$ ,  $|\epsilon|$  and  $\gamma$ . The solid line is the function  $F(x)/x$  given by Eq. (3).

#### 4. Results and Discussion

We now discuss the experiments that were carried out to observe the ratchet effect for  $\tau$ 's close to the quantum resonance at  $\ell = 1$  and for  $\tau \sim 0$  which is the

true classical limit [19]. The measurements involve the determination of the mean momentum of the kicked BECs for various combinations of the parameters  $q$ ,  $\phi_d$ ,  $\varepsilon$  and  $\gamma$ . The measured momentum was then scaled by  $-\phi_d q \sin \gamma$  and plotted as a function of the scaling variable  $x$  for  $\ell = 1$  (Fig. 2) and for  $\ell = 0$  (Fig. 3). In Fig. 2(a) and Fig. 3,  $x$  was changed by varying kick number,  $q$ , while in Fig. 2(b) different  $x$  were obtained by scanning either  $|\varepsilon|$  (red circles and green squares) or  $\phi_d$  (blue triangles). The solid line in both figures is a plot of the function  $\frac{F(x)}{x}$  given by Eq. (3). It can be seen that no matter how  $x$  is varied, the experimental results are in good agreement with the theory for many different combinations of parameters. An exception to this is seen in Fig. 3 at high  $x$  values. We postulate that this could be due to the lack of precision in the measurement of the kick strength. In addition, there is a regime over  $x$  where an inversion of the ratchet current takes place, with a maximum inversion at  $x \approx 5.6$ . Interestingly this reversal of the ratchet

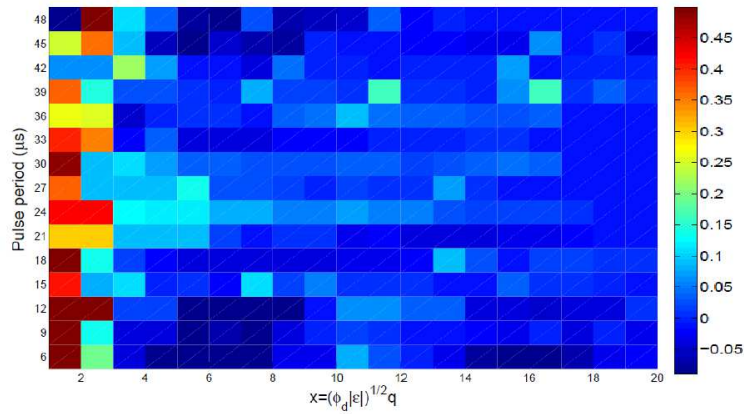


Fig. 4. False color plot of the mean momentum current as a function of scaling variable  $x$  (the  $x$ -axis) and pulse period (the  $y$ -axis). The color scale is the magnitude and direction of the mean momentum. The deep blue color represents the lowest value of mean momentum (negative in this case) showing the inversion region. Note that there is a momentum current inversion close to true classical and  $\varepsilon$ -classical (bottom and top on the  $y$ -axis respectively) regimes which disappears if one goes away from either (towards the region between  $\ell = 0$  and  $\ell = 1$ ).

takes place without altering any of the centers of symmetry of the system. Even though the  $\varepsilon$ -classical theory assumes  $|\varepsilon|$  is small, the experimental results show that it remains valid for higher values of  $|\varepsilon|$  as well. This is equally valid in the

true classical regime near  $\ell = 0$ . In fact the window of valid  $|\varepsilon|$  depends on the kick number [20], being rather large for small  $q \lesssim 10 - 15$ . This is expected from a Heisenberg/Fourier argument [19, 21, 26]. Since the time offset from QR effectively

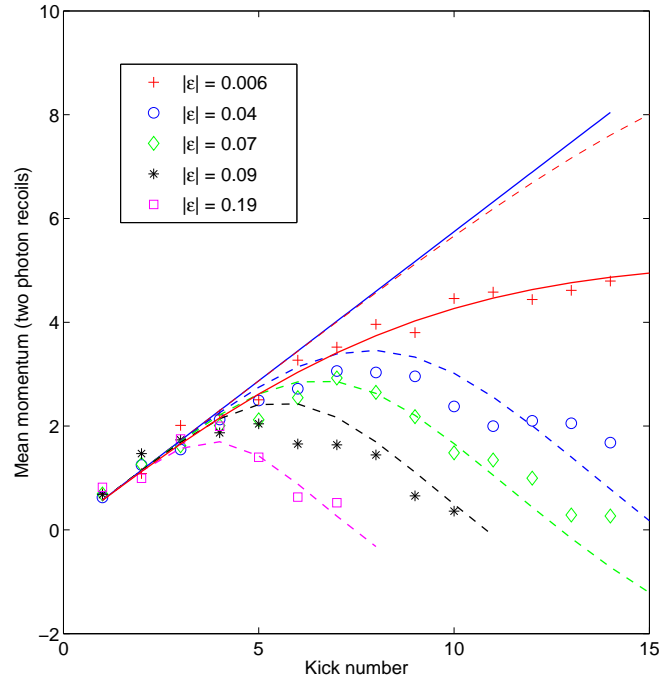


Fig. 5. Momentum current as a function of kick number for  $|\varepsilon| = 0.006$  (red crosses),  $|\varepsilon| = 0.04$  (blue circles),  $|\varepsilon| = 0.07$  (green diamonds),  $|\varepsilon| = 0.09$  (black stars) and  $|\varepsilon| = 0.19$  (purple squares). The blue solid line is the plot of  $\langle p_{q, res} \rangle = -\frac{\phi_d q}{2} \sin \gamma$  for  $\phi_d = 1.3$  and  $\gamma = -\pi/3$ . The dashed lines are the plot of Eq. (3) with corresponding  $|\varepsilon|$  and the red solid line is the plot of Eq.(2) in Ref. [8] for  $\beta = 0.5$  and  $\Delta\beta = 0.02$ .

defines a new Planck constant [5, 20], we can easily switch from the classical to the quantum regime by a simple change of the pulse period [27]. Figure 4 is a false color plot of scaled mean momentum for the pulse periods starting from close to true classical limit ( $\ell = 0$ ) up to the first quantum resonance ( $\ell = 1$ ). The data were collected by scanning over the kick number for the different pulse periods. The data presentation is such that the scaling variable  $x$  is on the  $x$ -axis, pulse periods are on the  $y$ -axis and the mean momentum is plotted on the color axis. The deep blue color represents negative scaled mean momentum. It can be clearly seen that, when the pulse periods are closer to the classical limit,  $\tau = 0$  (bottom of the  $y$ -axis) and to the first quantum resonance  $\tau = 2\pi$  i.e.  $T = 51.5\mu\text{s}$  (top of



the  $y$ -axis), we see the inversion of the momentum current. However the inversion becomes faint and disappears far away from either end (in the middle). Also visible near  $\tau = 0$  is a second region of inversion around  $x = 15$ . This is the same as the second inversion seen in Fig. 3

We also investigated the sensitivity of the the momentum transfer to the finite spread in initial quasi-momentum  $\Delta\beta$ . Figure 5 shows the plot of momentum current as a function of kick number for different values of  $|\varepsilon|$ . The solid blue line is the plot of  $\langle p_{q,res} \rangle = -\frac{\phi_d q}{2} \sin \gamma$ . The dashed lines are plots of Eq. (3) for the corresponding experimental parameters. The experimental results show that the farther one goes from resonance the sooner the momentum current turns towards negative values (current reversal). These results are in good agreement with the theory except very close to resonance, where the red dashed curve fits poorly to the red crosses. For this data, we note that the suppression in momentum current is likely to be caused mainly by the effect of the initial spread of quasi-momentum. This phenomenon was also seen in Ref. [8] where the ratchet current for finite  $\Delta\beta$  was shown to be  $\langle p_{q,res} \rangle_{\Delta\beta} = \frac{\phi_d}{2} \sum_{s=1}^q \sin[(\pi\ell + \tau\beta)s - \gamma] \exp[-2(\pi\ell\Delta\beta s)^2]$ . This equation with  $\Delta\beta = 0.02$  (independently estimated from time-of-flight measurements) is also plotted in Fig. 5 (red solid line). It can be seen to agree well with experiment. Thus for  $|\varepsilon| \gtrsim 0.04$  (corresponding to an offset from resonance of  $0.3 \mu s$ ),  $\Delta\beta$  plays an unimportant role in the dynamics of the ratchet. This is because at resonance the total phase the momentum states acquire must be an integer multiple of  $2\pi$ . Any deviation from this condition significantly suppresses the momentum current at longer times. However the momentum state phases away from resonance are already pseudo-random, so the phase changes caused by  $\Delta\beta$  have a negligible effect.

## 5. Conclusion

We have performed experiments to investigate several aspects of the off-resonant atomic ratchet by exposing an initial atomic state which was a superposition of two momentum states to a series of standing wave pulses. We measured the mean momentum current as a function of a scaling variable  $x$ , which contained important pulse parameters such as the offset of the kicking period from resonance, the kick number, and the kick strength both in true classical ( $\ell = 0$ ) and the  $\varepsilon$ - classical ( $\ell = 1$ ) regimes. We showed that a scaled version of the mean momentum in both cases could be described solely by  $x$ , a result postulated by a theory based on a classical treatment of the system [16]. The experiment verified that for certain ranges of  $x$  the momentum current exhibited an inversion. We showed that the true classical and  $\varepsilon$ - classical regimes essentially display the same behavior. However it should be noted that in the  $\ell = 0$  case, the amplitude of the ratchet current oscillations as a function of  $x$  are more pronounced and are a better match to the theory. We postulate that this is due to the fact that the short time between the pulses near  $\ell = 0$  provides little opportunity for dephasing effects from vibrations and spontaneous emission to become important. The experiment verified that for certain

ranges of  $x$  the momentum current exhibited an inversion. We also studied the effect of initial quasi-momentum width on the ratchet current away from resonance. This width has a large impact extremely close to resonance, but plays an unimportant role as we go only a little farther from resonance. Ultimately one can now control the strength and direction of the ratchet without changing the underlying relative symmetry between the initial state and the potential. In addition the crossover between classical and  $\varepsilon$ -classical dynamics was observed.

## 6. Acknowledgements

We thank Sandro Wimberger for fruitful discussions.

## References

- [1] F. L. Moore, J. C. Robinson, C. F. Bharucha, B. Sundaram, and M. G. Raizen, *Phys. Rev. Lett.* **75**, 4598 (1995).
- [2] F. L. Moore, J. C. Robinson, C. Bharucha, P. E. Williams, and M. G. Raizen, *Phys. Rev. Lett.* **73**, 2974 (1994).
- [3] C. Ryu, M. F. Anderson, A. Vaziri, M. B. d’Arcy, J. M. Grossman, K. Helmerson, and W. D. Phillips, *Phys. Rev. Lett.* **96**, 160403 (2006).
- [4] F. M. Izrailev, *Phys. Rep.* **196**, 299 (1990).
- [5] S. Fishman, I. Guarneri and L. Rebuzzini, *Phys. Rev. Lett.* **89**, 084101 (2002); *J. Stat. Phys.* **110**, 911 (2003).
- [6] G. Behinaein, V. Ramareddy, P. Ahmadi, and G. S. Summy, *Phys. Rev. Lett.* **97**, 244101 (2006); V. Ramareddy, G. Behinaein, I. Talukdar, P. Ahmadi and G. S. Summy, *Eur. Lett.* **89**, 33001 (2010); M. K. Oberthaler, R. M. Godun, M. B. d’Arcy, G. S. Summy, and K. Burnett, *Phys. Rev. Lett.* **83**, 4447 (1999).
- [7] T. S. Monteiro, P. A. Dando, N. Hutchings, M. Isherwood, *Phys. Rev. Lett.* **89**, 194102 (2002).
- [8] I. Dana, V. Ramareddy, I. Talkukdar, and G. S. Summy, *Phys. Rev. Lett.* **100**, 024103 (2008).
- [9] M. Sadgrove, M. Horikoshi, T. Sekimura and K. Nakagawa, *Eur. Phys. J. D* **45**, 229 (2007).
- [10] P. Reimann, *Phys. Rep.* **361**, 57 (2002); R. D. Astumian and P. Hänggi, *Phys. Today* **55**, No.11, 33 (2002).
- [11] M. Sadgrove, M. Horikoshi, T. Sekimura, and K. Nakagawa, *Phys. Rev. Lett.* **99**, 043002 (2007).
- [12] T. Salger, S. Kling, T. Hecking, C. Geckeler, L. M.-Molina, M. Weitz, *Science*, **326**, 1241 (2009).
- [13] I. Dana and V. Roitberg, *Phys. Rev. E* **76**, 015201(R) (2007).
- [14] E. Lundh and M. Wallin, *Phys. Rev. Lett.* **94**, 110603 (2005).
- [15] A. Wickenbrock, D. Cubero, N. A. Abdul Wahab, P. Phoonthong, F. Renzoni, *Phys. Rev. E* **84**, 021127 (2011).
- [16] M. Sadgrove and S. Wimberger, *New J. Phys.* **11**, 083027 (2009).
- [17] R. K. Shrestha, J. Ni, W. K. Lam, S. Wimberger, and G. S. Summy, *Phys. Rev. A* **86**, 043617 (2012).
- [18] I. Talukdar, R. Shrestha and G. S. Summy, *Phys. Rev. Lett.* **105**, 054103 (2010).
- [19] M. Sadgrove S. Wimberger, S. Parkins, and R. Leonhardt, *Phys. Rev. Lett.* **94**, 174103 (2005).

- [20] S. Wimberger, I. Guarneri and S. Fishman, *Nonlinearity* **16**, 1381 (2003).
- [21] S. Wimberger, M. Sadgrove, S. Parkins, and R. Leonhardt, *Phys. Rev. A* **71**, 053404 (2005).
- [22] G. Casati and I. Guarneri, *Commun. Math. Phys.* **95**, 121 (1984).
- [23] M. D. Barrett, J. A. Sauer, and M. S. Chapman, “All-Optical Formation of an Atomic Bose-Einstein Condensate”, *Phys. Rev. Lett.* **87**, 010404 (2001).
- [24] M. Lepers, V. Zehnlé and J. C. Garreau, *Phys. Rev. A* **77**, 043628 (2008).
- [25] L. Deng, E. W. Hagley, J. Denschlag, J. E. Simsarian, Mark Edwards, Charles W. Clark, K. Helmerson, S. L. Rolston, and W. D. Phillips, *Phys. Rev. Lett.* **83**, 5407 (1999).
- [26] M. Sadgrove and S. Wimberger, *Adv. At. Mol. Opt. Phys.* **60**, 315 (2011).
- [27] At QR there is effectively no evolution between the kicks, making the system formally equivalent to the situation where the pulse period and therefore the scaled Planck’s constant are zero.